NIH RELAIS Document Delivery

NIH-10289409

JEFFDUYN

NIH -- W1 RA354

JOZEF DUYN
10 Center Dirve
Bldg. 10/Rm.1L07
Bethesda, MD 20892-1150

ATTN:
PHONE: 301-594-7305
FAX: -
E-MAIL:

SUBMITTED: 2002-09-04 08:27:56
PRINTED: 2002-09-06 06:40:59
REQUEST NO.:NIH-10289409
SENT VIA: LOAN DOC
7999126

NIH Fiche to Paper Journal

TITLE: RADIOLOGY
PUBLISHER/PLACE: Radiological Society Of North America Easton Pa
VOLUME/ISSUE/PAGES:1992 Jun;183(3):711-8 711-8
DATE: 1992
AUTHOR OF ARTICLE: Duijn JH; Matson GB; Maudsley AA; Hugg JW; Weiner MW
TITLE OF ARTICLE: Human brain infarction: proton MR spectroscopy.
ISSN: 0033-8419
OTHER NOS/LETTERS: Library reports holding volume or year
0401260
1584925
SOURCE: PubMed
CALL NUMBER: W1 RA354
REQUESTER INFO: JEFFDUYN
DELIVERY: E-mail: jhd@helix.nih.gov
REPLY: Mail:

Jeffrey H. Duijn, PhD • Gerald B. Matson, PhD • Andrew A. Maudsley, PhD
James W. Hugg, PhD • Michael W. Weiner, MD

Human Brain Infarction: Proton MR Spectroscopy[1]

Two-dimensional proton magnetic resonance (MR) spectroscopic imaging studies were performed of the distributions of the major hydrogen-1 metabolites of choline, creatine, *N*-acetyl aspartate (NAA) and lactate in normal ($n = 6$) and subacutely to chronically infarcted ($n = 10$) human brain. The two dimensions of phase encoding were applied over a 20-mm-thick section of brain tissue that had been selected with a double spin-echo localization method. Normal brain showed bilaterally symmetric metabolite distributions and no detectable lactate. Nine of 10 studies of brain infarction showed substantial decreases in NAA, creatine, and choline in the infarcted area compared with control areas; averaged for all studies, the decreases were 77% ± 8, 63% ± 11, and 54% ± 12, respectively (mean ± standard error). The decreased metabolite concentrations are probably due primarily to diminished cell density in the infarct. The decrease in NAA was larger than the decreases in choline and creatine. Findings in all of the studies showed lactate in the infarcted tissue and/or ventricles. The continued presence of lactate in the infarct indicates increased anaerobic glycolysis due to ischemia or other factors.

Index terms: Brain, infarction, 10.781 • Brain, MR, 10.1214 • Magnetic resonance (MR), spectroscopy, 13.1229

Radiology 1992; 183:711–718

Over the past few years proton magnetic resonance (MR) spectroscopy has developed into a useful technique with which to monitor noninvasively the metabolite levels in normal and diseased human brain. Altered metabolite levels have been reported in cases of hyperventilation (1), acute (2–5) and chronic (4–10) brain infarction, demyelinating disease (11), brain tumors (12–16), epilepsy (17,18), acquired immunodeficiency syndrome (19), and multiple sclerosis (20–22). All studies of brain infarction showed marked changes in metabolite concentrations.

Findings in two studies of acute infarction (2,3) showed complete loss of nitrogen acetyl aspartate (NAA) and a reduction in choline and creatine; results of studies of acute infarction (2–5) showed a marked increase in lactate in the infarcted area. In studies of chronic infarction (4,6–9), the infarcted region exhibited loss of NAA, choline, and creatine. The loss of NAA is of particular interest because it has been suggested that NAA is largely localized in neurons (23); however, it has not yet been established whether NAA is located in other cells. Findings in one of the previously reported cases (6) showed increased lactate in brain tissue outside the infarcted area. Results in two of the previously reported chronic infarctions (9,10) showed persistent elevation in lactate up to 4 months after the infarction. The presence of persistent lactate indicates the occurrence of increased glycolysis, which might be a marker for ongoing ischemia or other processes.

Early hydrogen-1 MR spectroscopic techniques obtained metabolite spectra from a single localized volume, termed the volume of interest (VOI). Examples of these techniques are image-selected in vivo spectroscopy (24), stimulated-echo acquisition mode (25–28), spatially resolved spectroscopy (29), and the Carr-Purcell double spin-echo point-resolved spectroscopy volume selection technique (30,31). Recently, MR spectroscopic imaging methods, which use phase encoding over a selected VOI to obtain spectral data from multiple, adjacent voxels (32,33), have been applied to measure H-1 metabolites in human brain (12,14,17,34–37). The data can be presented as spectra from individual voxels or in an image format to view distributions of individual metabolites over the VOI.

In this article we present results of two-dimensional H-1 MR spectroscopy in human brain, with the goals of determining proton metabolite distributions in normal brain and of assessing the effects of brain infarction on these distributions.

MATERIALS AND METHODS

Human Subjects

Studies were performed of control subjects ($n = 6$) aged 25–50 years and of patients with nonhemorrhagic cerebral infarcts ($n = 10$) (Table 1). All subjects provided informed consent as approved by the Human Research Committee, University of California, San Francisco.

MR Imaging and MR Spectroscopy

Experiments were performed on an imager (Gyroscan S15; Philips Medical Systems North America, Shelton, Conn) op-

[1] From the Magnetic Resonance Unit, Department of Veterans Affairs Medical Center (11M), 4150 Clement St, San Francisco, CA 94121 (J.H.D., G.B.M., A.A.M., J.W.H., M.W.W.), and the Departments of Pharmaceutical Chemistry (G.B.M.), Radiology (A.A.M., M.W.W.), and Medicine (M.W.W.), and the Cardiovascular Research Institute (J.W.H.), University of California, San Francisco. Received May 9, 1991; revision requested July 8; final revision received January 13, 1992; accepted February 3. Supported in part by the Department of Veterans Affairs Medical Research Service; by National Institutes of Health grants R01 DK33293, 1R01 CA48815, and HL07192; and by Philips Medical Systems.
Address reprint requests to J.H.D.

Abbreviations: NAA = *N*-acetyl aspartate, VOI = volume of interest.

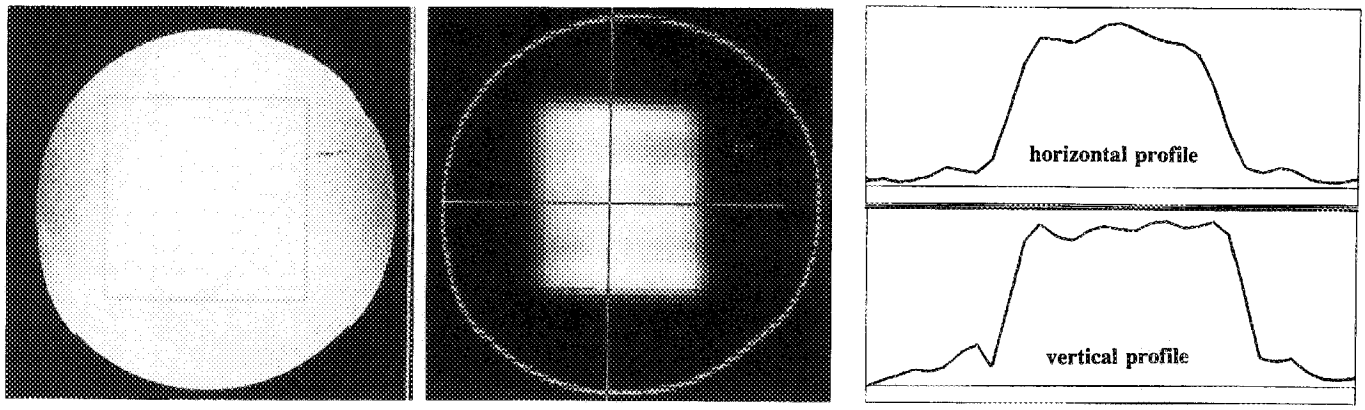

Figure 2. H-1 MR spectroscopic measurement of spherical 3-L phantom containing a gelatin with 20 mmol/L lactate. **(a)** Transverse MR image shows 90 × 90 × 20-mm (anteroposterior × left to right × craniocaudal) VOI. **(b)** Lactate image is overlaid with edge-detected MR image. Horizontal and vertical lines give positions where image profiles in c were measured. **(c)** Horizontal (left to right) and vertical (anteroposterior) image profiles were measured along lines indicated in b.

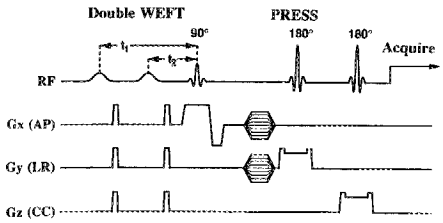

Figure 1. Acquisition scheme of H-1 MR spectroscopic experiment. The first part of the pulse sequence consisted of a double water elimination Fourier transform sequence for water suppression; t_1 and t_2 indicate inversion delay times. The second part of the pulse sequence was a point-resolved spectroscopy double spin-echo sequence (90°–180°–180°) for volume selection. The acquisition interval began shortly after the last gradient spoiler pulse. *Gx(AP)* = magnetic field gradient in anteroposterior plane, *Gy(LR)* = magnetic field gradient in left-right plane, *Gz(CC)* = magnetic field gradient in craniocaudal plane, *PRESS* = point-resolved spectroscopy, *RF* = radio frequency, *WEFT* = water elimination Fourier transform.

Table 1
Selection of Subjects with Brain Infarction

Patient/ Age (y)	Distribution of Infarct*	Infarct Size (cm)†	Infarct Age (d)
1/83	Right PCA	>4	600
2/70	Posterior division right MCA	>4	300
3/72	Right PCA-MCA border zone	2–4	400
4/67	Left MCA parietal	>4	1,400
5/54	Right parietal deep white matter	2–4	200
6/63	Left thalamus striate artery	<2	5
7/79	Anterior division right MCA	2–4	10
8/75	Right MCA	>4	400
9/76	Right MCA	>4	600
10/76	Left MCA	>4	700

* MCA = middle cerebral artery, PCA = posterior cerebral artery.
† Maximum infarct diameter.

erating at 2.0 T, with the standard spectroscopy acquisition software. The point-resolved spectroscopy sequence (30,31) was used for VOI selection (Fig 1), with section-selective pulses in anteroposterior, left-right, and craniocaudal directions; gradient phase encoding (32,33) was performed over two dimensions. The first part of the pulse sequence of Figure 1 is a double water elimination Fourier transform sequence consisting of adiabatic inversion pulses for water suppression (38).

Procedure

A standard set of sagittal (repetition time = 450 msec, echo time = 30 msec [450/30] and transverse (2,000/30, 90) MR images was obtained. For the MR spectroscopic study, a 20-mm-thick transverse section within the brain was selected with further in-plane volume selection of typical dimensions of 100 × 100 mm. In a number of studies with both MR imaging and MR spectroscopy, transverse sections were angulated by approximately 40° to reduce contamination with lipid (see below). For water suppression, water elimination Fourier transform delay times t_1 and t_2 (Fig 1) were close to 800 msec and 50 msec, respectively. A 16 × 16 phase-encoding MR spectroscopic experiment was performed over a typical field of view of 180 × 180 mm. Other relevant parameters were repetition time of 2,000 msec, echo time of 272 msec, four signals averaged, 512 time points, and a sampling bandwidth of 1,000 Hz. The sampling was initiated so that 21% of the sampling interval occurred before the echo top.

Data Processing

A 1-Hz exponential line broadening was applied in the time domain, and both spatial dimensions were exponentially line broadened by approximately 1 mm, resulting in an in-plane resolution of approximately 1.2 cm, with a voxel size of 2.9 cm^3. In studies involving high levels of water and/or lipid contamination (three of the 16 studies), a Hamming filter (39) was used, resulting in an in-plane resolution of approximately 1.6 cm and a voxel size of approximately 5 cm^3. The two-dimensional MR spectroscopic images were created by integration over selected spectral regions with use of custom display software (40). In addition, the software enabled extraction of magnitude spectra by summing (interpolated) voxels within selected spatial regions. These regions were usually selected based on findings in the MR spectroscopic image of NAA (32 × 32 matrix). To minimize contamination from other tissues, whenever possible spectra were extracted from regions well inside a specific tissue region (infarcted brain, normal brain, or ventricles). Gaussian peaks were fitted to the resonances of choline, creatine, and NAA. When lactate also appeared in a spectrum, two additional gaussian peaks were fitted to this resonance, which in most cases was only partially resolved into a doublet. Peak fitting was usually successful at a signal-to-noise ratio greater than 2–3. The estimated detectability limit for single voxels of our technique was approximately 3.00 mmol/L for the doublet of lactate (one CH_3 group), 2.0 mmol/L for the singlet resonances of creatine and NAA (one CH_3 group), and approximately 0.7 mmol/L for choline (three CH_3 groups).

The images of lactate, created by inte-

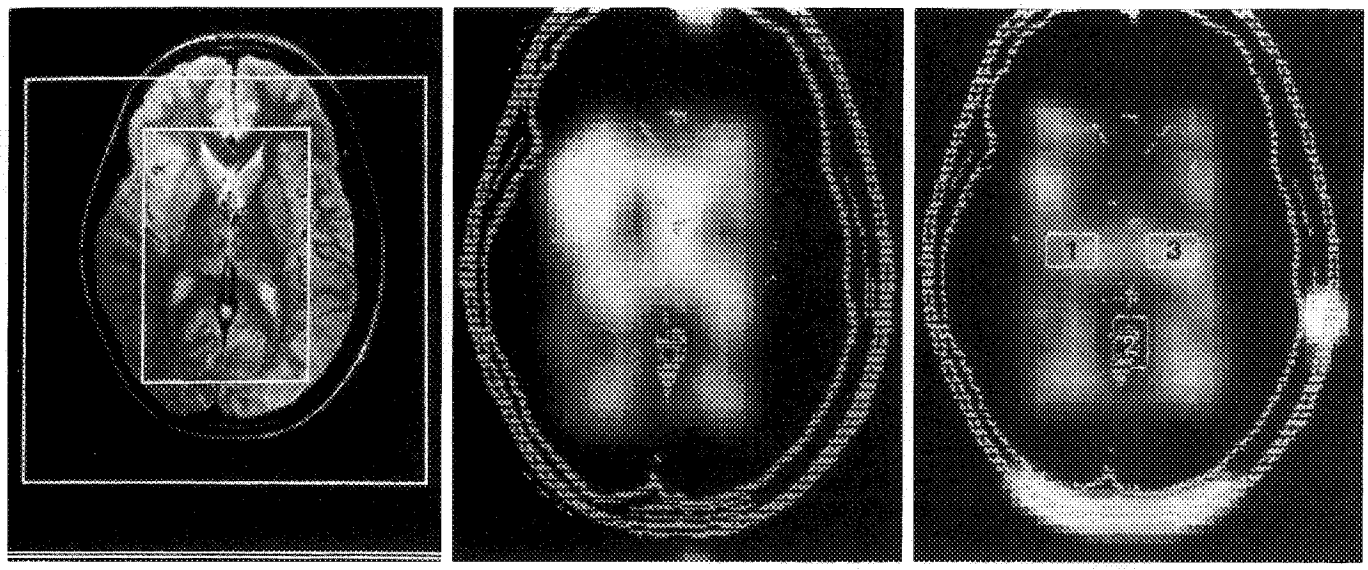

a. b. c.

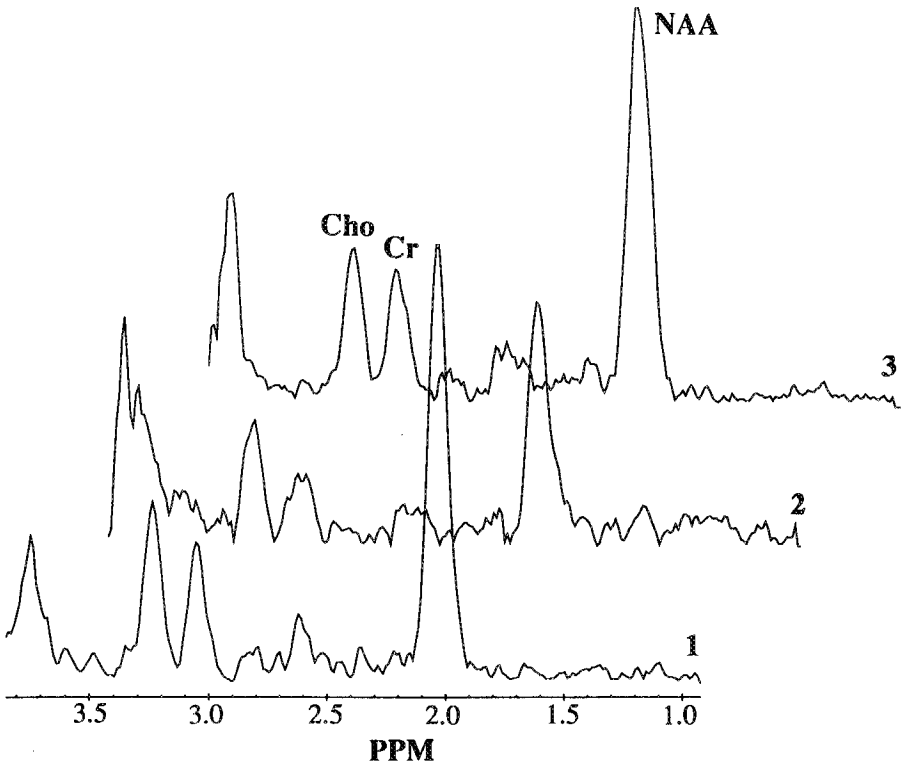

d.

Figure 3. H-1 MR spectroscopic measurement of 25-year-old healthy subject. **(a)** Six-millimeter-thick, transverse, T2-weighted MR image shows 120 × 90 × 20-mm (anteroposterior × left to right × craniocaudal) VOI (inner box) and 180 × 180-mm field of view (outer box). **(b)** Choline-plus-creatine metabolite image is overlaid with high-pass filtered MR image. **(c)** NAA-metabolite image overlaid with high-pass filtered MR image shows regions from which spectra were obtained. *1* = contralateral brain, *2* = ventricles, *3* = infarct. **(d)** H-1 spectra were obtained from regions indicated in c. Each spectrum was obtained from approximately 9 mL of tissue.

gration over a spectral region of 1.26–1.40 ppm, were often contaminated with lipid signal originating from the scalp and the bone marrow; nevertheless, these images are termed "lactate" images. The spectral region covered by the broad lipid resonances (1.0–2.5 ppm) included the lactate region and prohibited reliable quantitation of lactate. Intensity within the VOI of the lactate image usually originated from lactate, whereas intensity outside the VOI represented mostly lipid. This was verified by examining spectra extracted from high-intensity regions: Spectra from within the VOI usually showed a doublet at 1.33 ppm, whereas spectra from outside the VOI showed a very broad resonance around this chemical shift.

RESULTS

An MR spectroscopic experiment on a 3-L spherical phantom (20 mmol/L lactate) (Fig 2) showed intensity variations of about 10%, largely due to Gibbs ringing and imperfections in the volume selection. The accuracy of metabolite measurements in human brain (see below), in which the signal-to-noise ratio was lower, was therefore not better than approximately 10%.

The results of an MR spectroscopic study of a healthy volunteer are displayed in Figure 3. Figure 3a displays the T2-weighted MR image of a 6-mm-thick transverse section, along with two box outlines; the smaller box indicates the VOI for the MR spectroscopic experiment, while the larger box shows the field of view over which phase encoding was performed. Metabolite distributions are indicated in the MR spectroscopic images of Figure 3b and 3c. These latter figures are overlaid with a high-pass filtered MR image of Figure 3a to facilitate identification of anatomic features on the MR spectroscopic image. Figure 3b shows the image of the sum of choline and creatine. The NAA spectroscopic image is displayed in Figure 3c; spectra extracted from the regions indicated on the image are shown in Figure 3d. The middle spectrum, extracted from an area containing cerebrospinal fluid, shows clearly reduced metabolite concentrations. Some metabolite resonance intensity remains in this spectrum due to the fact that the MR spectroscopic imaging voxel (20 mm thick) contains some brain tissue not displayed on the thin-section (6-mm-thick) MR image.

Two different H-1 MR spectroscopic studies of infarcted brain are

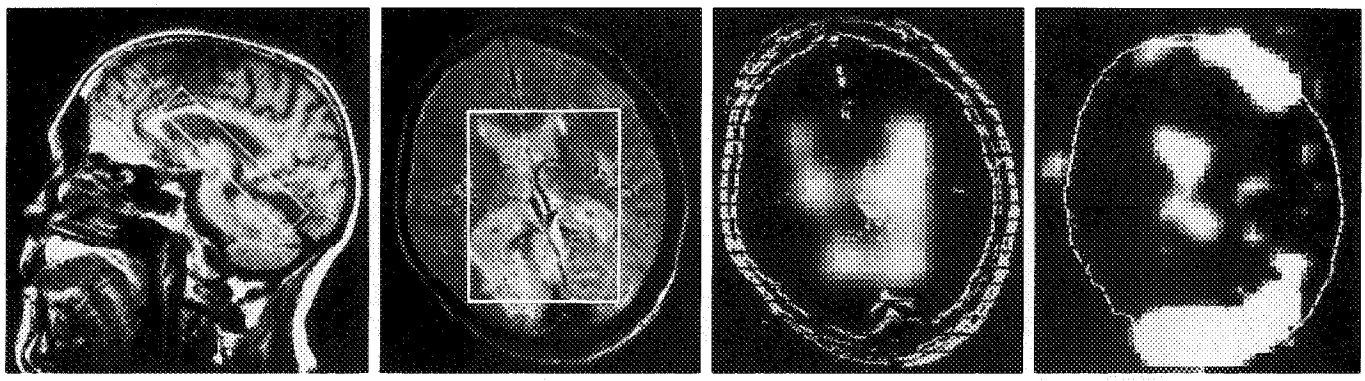

a. b. c. d.

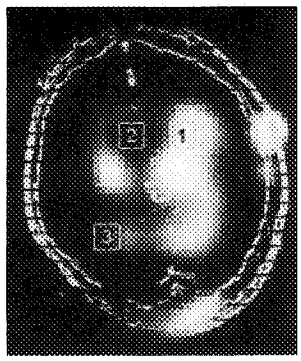

e.

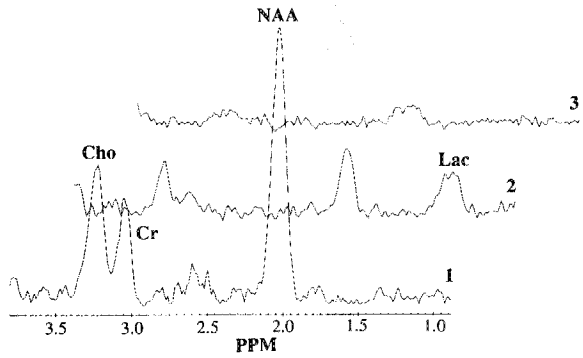

f.

Figure 4. Patient 1. H-1 MR spectroscopic measurement of brain infarction was made with use of angulation. **(a)** Seven-millimeter-thick sagittal T1-weighted MR image shows (angulated) VOI. **(b)** Six-millimeter-thick transverse (angulated), T2-weighted (echo time = 50 msec) MR image shows VOI. **(c)** Choline-plus-creatine metabolite image is overlaid with high-pass filtered MR image. **(d)** Lactate metabolite image is overlaid with edge-detected MR image. **(e)** NAA metabolite image overlaid with high-pass filtered MR image shows regions from which spectra were obtained. *1* = contralateral brain, *2* = ventricles, *3* = infarct. **(f)** H-1 spectra were obtained from regions indicated in **e.** Each spectrum was obtained from approximately 10 mL of tissue.

displayed in Figures 4 and 5. In the case of Figure 4 (patient 1), the transverse MR image sections and the MR spectroscopic section were angulated. Figure 4a depicts the MR spectroscopic VOI and indicates the angulation. The T2-weighted transverse section displayed in Figure 4b shows the infarcted region as a large area of hyperintensity in the right occipital lobe, posterior to the ventricle. Figure 4b displays the MR spectroscopic VOI. The choline-plus-creatine MR spectroscopic image for patient 1 (Fig 4c), with an overlay of the high-pass filtered MR image, shows reduction in the signal of choline plus creatine in the ventricles, as well as in the infarct region. Figure 4d shows a lactate MR spectroscopic image of patient 1; that image is overlaid with an outline from the MR image. The lactate is displayed as hyperintensity within the VOI, while hyperintensity outside the VOI (regions near the skull) represents lipid, as verified with spectra obtained from these regions (not shown). Comparison with the MR image shows that lactate originates from within the ventricles; increased lactate concentration was not observed in the infarct.

The lipid signal does not appear as a continuous rim around the brain for the following reasons. First, to create the lactate image, only a small spectral region (1.26–1.40 ppm) was selected for integration. The signal from lipid surrounding the skull is very broad (1.0–2.5 ppm), partly because the area outside the VOI was not well shimmed, since localized shimming was performed. Thus, the lipid contribution to the integrated region was highly variable. Second, the lipids were highly suppressed by the localization scheme employed to select the VOI. The degree of lipid suppression depended on the section-selection profiles of the point-resolved spectroscopy pulses and the position of the lipid with respect to the edges of the VOI. Thus, the amount of lipid that was still detected with the point-resolved spectroscopy localization was spatially quite variable.

The NAA MR spectroscopic image for patient 1 is displayed in Figure 4e. As in Figure 4d, hyperintensity outside the VOI represents lipid. Similar to findings with choline plus creatine, NAA was markedly reduced within the ventricles and within the infarct. Voxels within the regions labeled *1*, *2*, and *3* on Figure 4e (representing normal-appearing contralateral brain, ventricle, and infarct, respectively) were summed, and the resulting spectra are displayed in Figure 4f. The spectrum from region 1 shows the expected resonances of choline, creatine, and NAA. The spectrum of region 2 shows the presence of lactate, along with much reduced levels of NAA, choline, and creatine. As discussed previously, the levels of NAA, choline, and creatine probably arise from tissue above or below the ventricles that is not seen on the thin-section (6-mm-thick) MR image. No pronounced metabolite resonances are observed in region 3.

Figure 5 shows the MR spectroscopic results for patient 6. Figure 5a shows the MR image indicating the VOI (inner box). The infarct area appears as a small hyperintense region in the left hemisphere, close to the ventricles. The lactate image (Fig 5b) shows a hyperintense region at the same location. As in Figures 4d and 4e, hyperintensity outside the VOI represents lipid. A spectrum (Fig 5c) obtained from the hyperintense region in the lactate image shows a partially resolved doublet at 1.33 ppm; that spectrum was identified as lactate. The spectrum also shows the resonances of choline, creatine, and NAA. Owing to the small size of the stroke region, part of these metabolite signal intensities originates from tissue surrounding the infarct.

The results of analyses of the spectra obtained from different regions in

Table 2
H-1 MR Spectroscopic Data from Normal Brain and from Brain Infarctions

Subjects	Choline/ NAA*	Creatine/ NAA*	Choline†	Creatine†	NAA†	Lactate/ NAA‡	Lactate/ NAA§
Healthy (n = 6)							
Mean ± standard error	0.43 ± 0.03	0.29 ± 0.02	1.02 ± 0.05	1.04 ± 0.03	1.05 ± 0.06	NA	NA
Patients							
1	...	...	...	...	...	...	0.22
2	0.96	0.49	0.33	0.22	0.13	...	0.11
3	0.59	0.38	0.56	0.54	0.40	...	0.27
4	...	...	...	...	...	...	0.08
5	1.20	0.50	0.95	0.68	0.38	0.10	0.09
6	0.60	0.39	1.06	1.10	0.89	0.28	...
7	1.24	0.49	0.75	0.42	0.21	0.18	0.20
8	1.10	0.63	0.68	0.55	0.29	0.17	0.18
9	...	...	...	...	..	0.13	0.22
10	1.08	0.73	0.23	0.21	0.10	0.06	0.13
Mean ± standard error	0.97 ± 0.15	0.51 ± 0.07	0.46 ± 0.12	0.37 ± 0.11	0.23 ± 0.08	0.09 ± 0.03	0.15 ± 0.03
P‖ (unpaired t test)	< .001	.005	< .001	< .001	.001	NA	NA

* In patients, spectra were extracted from infarcted brain.
† In healthy subjects, numbers are metabolite ratios in spectra from left and right hemispheres; in patients, numbers are metabolite ratios in spectra from infarcted and normal brain.
‡ Metabolite ratio of infarcted versus normal spectra. Estimated measurement error = 0.04–0.08 (see text).
§ Metabolite ratio of ventricular versus normal spectra. Estimated measurement error = 0.04–0.08 (see text).
‖ Significance of infarcted to normal brain.

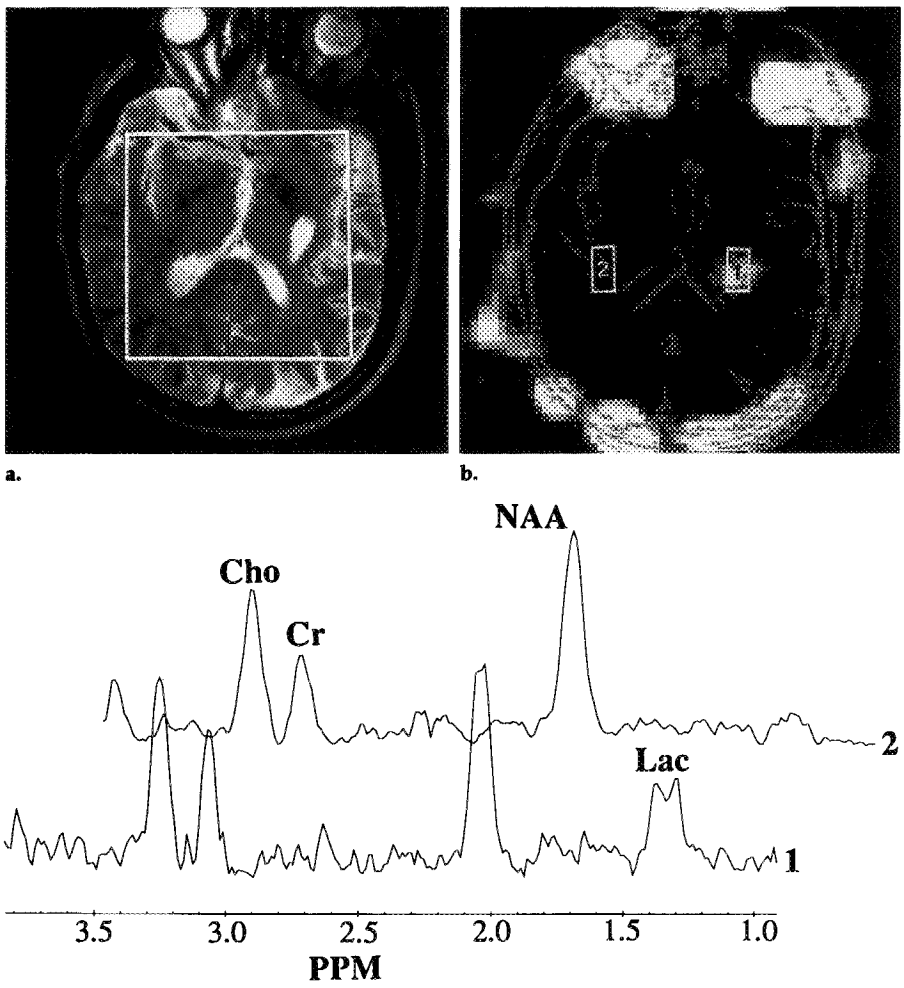

Figure 5. Patient 6. H-1 MR spectroscopic measurement of brain infarction. **(a)** Six-millimeter-thick transverse (not angulated), T2-weighted (echo time = 50 msec) MR image shows VOI. **(b)** Lactate metabolite image overlaid with high-pass filtered MR image shows regions from which spectra were obtained (*1*, *2*). (c) H-1 spectra were obtained from regions indicated in **b.** Each spectrum was obtained from approximately 9 mL of tissue.

normal and infarcted brain are summarized in Table 2. Actual volumes ranged from 7 to 15 mL. Averaged ratios are presented as mean ± standard error. Mean ratios for choline/NAA and creatine/NAA obtained from healthy subjects were 0.43 ± 0.03 and 0.29 ± 0.02, respectively. Table 2 shows left-right ratios close to unity, indicating bilateral symmetry for choline, creatine, and NAA metabolite distributions in healthy subjects.

The infarct data are presented as levels of choline/NAA, creatine/NAA, and metabolites within the infarct compared with findings in normal-appearing contralateral brain. Lactate levels in the infarct and in the ventricles are compared to NAA in the contralateral region. All infarcts except one showed decreases of choline, creatine, and NAA in the infarct and a greater loss of NAA than of choline and creatine. The one exception was a very small infarct in patient 6 that demonstrated metabolite levels that were maintained probably because of contamination with surrounding normal tissue. Mean values of choline/NAA and creatine/NAA in the infarct were 0.97 ± 0.15 and 0.51 ± 0.07, respectively; these values were significantly higher than normal values ($P < .001$, $P < .03$, respectively). Within the infarct, choline, creatine, and NAA were reduced to 0.46 ± 0.12, 0.37 ± 0.11, and 0.23 ± 0.08, respec-

tively, compared with values in the contralateral normal-appearing region. Furthermore, the reduction in NAA was significantly greater than the reduction in either choline or creatine ($P < .001$ with paired t test). In the infarctions, the values for choline/NAA and creatine/NAA in contralateral normal tissue (0.47 ± 0.03 and 0.31 ± 0.01, respectively [not in Table 2]) were similar to the values found in healthy subjects.

No lactate was found in the healthy subjects. In six infarctions, lactate was found within the infarct. The last two columns of Table 2 (lactate/NAA) show that detectable levels of lactate were associated with all infarctions as measured in the infarct, within the ventricles, or both. The estimated error in the lactate/NAA ratio data is quite large (0.04–0.08) due to poor signal-to-noise ratio and to possible contamination with lipid signal. Therefore, care has to be taken with interpretation of these data.

DISCUSSION

Clinical Implications

There were three major findings in these experiments: Brain infarction was associated with a marked lowering in the level of observed H-1 metabolites at MR imaging compared with findings on the contralateral side, NAA was reduced to a greater extent than were choline and creatine, and all of the 10 subacute to chronic infarctions demonstrated persistent elevations in levels of lactate within the infarct and/or ventricles. The finding that the levels of H-1 metabolites were reduced in infarcts is consistent with findings in previous studies with both H-1 (2,3,7,8) and phosphorus-31 (41,42) MR spectroscopy.

Brain infarctions are associated with a marked decrease of cellular density in the region of the infarct (43), which largely accounts for the reduced metabolite concentrations. The finding that the ratios of choline/NAA and creatine/NAA were increased in the region of the infarct, as previously reported (7,8), is clearly due to a greater reduction in NAA than in choline or creatine. This is evidenced by the finding (Table 2) that the NAA concentration was reduced to 23% of its contralateral value, which is significantly ($P < .001$) more than the reductions in choline (to 46%) and creatine (to 37%). It has been suggested that NAA is specific to neurons (23). Thus the finding that NAA was reduced to a greater extent than were choline and creatine is consistent with the view that within the infarct there was a greater loss of neurons than of glial cells.

The finding that all of the subjects with subacute and chronic infarctions had persistent elevation in lactate levels is important. Previously, in a case report, Ott et al suggested that lactate concentrations may be elevated within or adjacent to subacute and chronic infarction (4); the current observations substantiate those findings. One possible explanation is that increased lactate concentrations represent continuing ischemia in the border zone of the infarction, sometimes referred to as ischemic penumbra (44). Although this remains a possibility, none of the cases showed increased lactate exclusively in the border zone of the infarct. Lactate was found within the infarcted area, within the ventricles, and, in some cases, in both.

The mechanism of the persistently elevated lactate level remains speculative. One study of a 32-day-old infarction used carbon-13–labeled glucose to show continued lactate turnover, demonstrating continued synthesis rather than simple loculation of a stagnant pool (9). One possible explanation is that the lactate is produced by viable yet persistently ischemic tissue. A second possible explanation is that lactate is produced by phagocytic glial cells or leukocytes in the infarct because of the known high rate of anaerobic glycolysis by these cells (45,46). A third possible explanation is that factors other than ischemia stimulate glycolysis of the tissue within the infarct.

While in the majority of cases the lactate was unambiguously identified by its chemical shift and characteristic doublet, in a few cases the doublet was not clearly evident due to low signal-to-noise ratio and suboptimal shimming. In these cases it was not possible to rule out the possibility that mobile lipids gave rise to the resonance. However, the narrowness of the resonance and the fact that the resonance occurred at the point of chemical shift for lactate and under circumstances in which lactate was observed in other subjects are findings that do not support the likelihood that mobile lipids give rise to this resonance.

Previous H-1 and P-31 MR spectroscopic studies with use of single-volume techniques obtained spectral information from only a single region. A major advantage of the MR spectroscopic technique is that signals are obtained simultaneously from multiple voxels within a relatively large VOI so that the spectra obtained from within the infarct can be directly compared with corresponding spectra from the contralateral region of brain. With this approach, the extent to which metabolite concentrations are reduced in the infarcted region can be estimated with the assumption that the contralateral brain is normal. Although our results indicate similar metabolite ratios in brains of healthy subjects and in regions of normal brain in the much older patients with brain infarctions, it is possible that aging affects H-1 metabolite concentrations in normal-appearing brain or that the healthy subjects had widespread vascular disease or other pathologic abnormalities that resulted in altered metabolite concentrations. Until H-1 MR spectroscopic data can be used to obtain quantitative estimates of molar concentrations of metabolites (47–51), it will not be possible to determine rigorously the extent of reductions produced by infarctions.

Limitations

A number of difficulties were encountered in the studies reported herein that are associated with obtaining quantitative results with MR spectroscopic methods.

A major problem encountered with in vivo H-1 MR spectroscopy is the presence of intense signals from water and lipid, especially in spectra acquired from regions close to the skull, which can interfere with correct interpretation of the signal intensities of choline, creatine, NAA, and lactate. Therefore, for the quantitation of lactate, spectra were examined from high-intensity regions in the lactate image. Lactate was identified as a relatively narrow doublet with 7-Hz splitting, while lipid was characterized as a broad resonance covering a frequency range of approximately 1.0–2.5 ppm.

During switching of B_0 gradients, eddy currents are induced in the conductive parts of the magnet (eg, cryostat), and the currents can cause some gradient to persist after the gradient pulses have been turned off. These eddy currents can potentially cause line broadening, phase distortion, section tilting, and artifacts in the section profiles. The line broadening was minimized by using the gradient producing the least residual eddy current as the last selection-spoiler gradient in the MR spectroscopic sequence (Fig 1). With an echo time of 272 msec, the

line broadening due to eddy currents was estimated to be less than 1 Hz over the VOI. Eddy currents can also give the transverse spins a net dephasing at the position of the echo top; the amount of dephasing depends on spatial position and is difficult to correct. Therefore, magnitude spectra were used for reconstruction of MR spectroscopic images and for summation of spectra obtained from multiple voxels.

Owing to the frequency offset between the different resonances in a spectrum, the VOI positions (but not the voxel positions) are offset for the different metabolites. The shift can cause spurious differences in amplitudes of metabolites when comparisons among different metabolites are made near the edge of the VOI. Therefore, data were not taken near the edges.

In addition to resulting in spatially inhomogeneous signal reception, inhomogeneity of the B_1 field can cause deterioration of the water suppression and degradation of the section profiles. ■

Acknowledgments: The authors gratefully acknowledge the contributions and assistance provided by D. C. Sorrel, MD, from the Letterman Army Medical Center; S. H. Graham, MD, PhD, from the San Francisco Department of Medical Affairs Medical Center; and J. Tsuruda, MD, from the University of California San Francisco.

References

1. Van Ryen PC, Luyten PR, Berkelbach van der Sprenkel JW, et al. 1H and 31P NMR measurement of cerebral lactate, high energy phosphate levels and pH in humans during voluntary hyperventilation: associated EEG, capnographic, and Doppler findings. Magn Reson Med 1989; 10:182–193.
2. Bruhn H, Frahm J, Gyngell ML, Merboldt KD, Haenicke KW, Sauter R. Cerebral metabolism of man after acute stroke: new observations using localized proton NMR spectroscopy. Magn Reson Med 1989; 9:126–131.
3. Umeda M, Eguchi T, Iai S, et al. The comparison of the lactate level of the human brain with disease using localized ^{1}H NMR spectroscopy (abstr). In: Book of abstracts: Society of Magnetic Resonance in Medicine 1990. Berkeley, Calif: Society of Magnetic Resonance in Medicine, 1990; 988.
4. Ott D, Ernst T, Hennig J. In vivo ^{1}H spectroscopy in cerebral ischemia (abstr). In: Book of abstracts: Society of Magnetic Resonance in Medicine 1990. Berkeley, Calif: Society of Magnetic Resonance in Medicine, 1990; 1011.
5. Luyten PR, van Ryen PC, Tulleken CAF, den Hollander JA. Metabolite mapping using ^{1}H NMR spectroscopic imaging in patients with cerebrovascular disease (abstr). In: Book of abstracts: Society of Magnetic Resonance in Medicine 1989. Berkeley, Calif: Society of Magnetic Resonance in Medicine, 1989; 452.
6. Berkelbach van der Sprenkel JW, Luyten PR, van Ryen PC, Tulleken CAF, den Hollander JA. Cerebral lactate detected by regional proton magnetic resonance spectroscopy in a patient with cerebral infarction. Stroke 1988; 19:1556–1560.
7. Hetherington H, Sappey-Marinier D, Hubesch B, Deicken R, Fein G, Weiner MW. Characterization of tissue metabolites in chronic strokes and deep white matter lesions by localized ^{1}H MRS (abstr). In: Book of abstracts: Society of Magnetic Resonance in Medicine 1989. Berkeley, Calif: Society of Magnetic Resonance in Medicine, 1989; 446.
8. Hubesch B, Sappey-Marinier D, Hetherington HP, et al. Clinical MRS studies of the brain. Invest Radiol 1989; 24:1039–1042.
9. Rothman DL, Howseman AM, Graham GD, et al. Observation of lactate turnover in infarcted human brain with 1-13C glucose infusion and 1H (abstr). In: Book of abstracts: Society of Magnetic Resonance in Medicine 1990. Berkeley, Calif: Society of Magnetic Resonance in Medicine, 1990; 107.
10. Howseman AM, Graham GD, Rothman DL, et al. A 1H NMR study of cerebral lactate distribution following stroke (abstr). In: Works in progress; Society of Magnetic Resonance in Medicine 1990. Berkeley, Calif: Society of Magnetic Resonance in Medicine, 1990; 1206.
11. Luyten PR, den Hollander JA, Marjos S, van den Knapp S, Valk J. In vivo 31P and 1H spectroscopy in patients with white matter disorders (abstr). In: Book of abstracts: Society of Magnetic Resonance in Medicine 1988. Berkeley, Calif: Society of Magnetic Resonance in Medicine, 1988; 257.
12. Luyten PR, Marien AJH, Heindel W, et al. Metabolic imaging of patients with intracranial tumors: H-1 MR spectroscopic imaging and PET. Radiology 1990; 176:791–799.
13. Langkowski JH, Wieland J, Bomsdorf H, et al. Pre-operative localized in vivo proton spectroscopy in cerebral tumors at 4.0 tesla: first results. Magn Reson Imaging 1989; 7:547–555.
14. Segebarth CM, Baleriaux DF, Luyten PR, den Hollander JA. Detection of metabolic heterogeneity of human intracranial tumors in vivo by 1H NMR spectroscopic imaging. Magn Reson Med 1990; 13:62–76.
15. Alger JR, Frank JA, Bizzi A, et al. Metabolism of human gliomas: assessment with 1-H MR spectroscopy and F-18 fluorodeoxyglucose PET. Radiology 1990; 177:633–641.
16. Bruhn H, Frahm J, Gyngell ML, et al. Noninvasive differentiation of tumors with use of localized H-1 MR spectroscopy in vivo: initial experience in patients with cerebral tumors. Radiology 1989; 172:541–548.
17. Luyten PR, van Rijen PC, Meinert LC, Marien AJH, den Hollander JA. Identifying epileptic foci by 1H NMR spectroscopic imaging in patients with therapy resistant epilepsy (abstr). In: Book of abstracts: Society of Magnetic Resonance in Medicine 1990. Berkeley, Calif: Society of Magnetic Resonance in Medicine, 1990; 1009.
18. Matthews PM, Andermann F, Arnold DL. A proton magnetic resonance spectroscopy study of focal epilepsy in humans. Neurology 1990; 40:985–989.
19. Menon DK, Baudouin CJ, Tomlinson D, Hoyle C. Proton MR spectroscopy and imaging of the brain in AIDS: evidence of neuronal loss in regions that appear normal with imaging. J Comput Assist Tomogr 1990; 14:882–885.
20. Christiansen P, Larsson HBW, Frederiksen J, Jensen M, Henriksen O. Localized in vivo proton spectroscopy in the brain of patients with multiple sclerosis (abstr). In: Book of abstracts; Society of Magnetic Resonance in Medicine 1990. Berkeley, Calif: Society of Magnetic Resonance in Medicine, 1990; 109.
21. Arnold DL, Matthews PM, Mollevanger L, Luyten P, Francis G, Antel J. In vivo localized proton magnetic resonance spectroscopy allows plaque characterization in multiple sclerosis (abstr). In: Book of abstracts; Society of Magnetic Resonance in Medicine 1990. Berkeley, Calif: Society of Magnetic Resonance in Medicine, 1990; 110.
22. Wolinsky JS, Ponnada A, Narayana, Fenstermacher MJ. Proton magnetic resonance spectroscopy in multiple sclerosis. Neurology 1990; 40:1764–1769.
23. Nadler JV, Cooper JR. *N*-acetyl-L-aspartic acid content of human neural tumours and bovine peripheral nervous tissues. J Neurochem 1972; 19:313–319.
24. Ordidge RJ, Connelly A, Lohman JAB. Image selected in vivo spectroscopy (ISIS): a new technique for spatially selective NMR spectroscopy. J Magn Reson 1986; 66:283–294.
25. McKinnon G. Volume selective excitation spectroscopy using the stimulated echo (abstr). In: Works in progress; Society of Magnetic Resonance in Medicine 1986. Berkeley, Calif: Society of Magnetic Resonance in Medicine, 1986; 168.
26. Granot J. Selected volume excitation using stimulated echoes (VEST): applications to spatially localized spectroscopy and imaging. J Magn Reson 1986; 70:488–492.
27. Kimmich R, Hoepfel D. Volume-selective multipulse spin-echo spectroscopy and imaging. J Magn Reson 1987; 72:379–384.
28. Frahm J, Merboldt KD, Haenicke W. Localized proton spectroscopy using stimulated echoes. J Magn Reson 1987; 72:502–508.
29. Luyten PR, Marien AJH, Sijtsma B, den Hollander JA. Solvent-suppressed spatially resolved spectroscopy: an approach to high-resolution NMR on a whole-body MR system. J Magn Reson 1986; 67:148–155.
30. Ordidge RJ, Bendall MR, Gordon RE, Connely A. Volume selection for in-vivo spectroscopy. In: Govil G, Khetrapal CL, Saran A, eds. Magnetic resonance in biology and medicine. New Delhi: Tata-McGraw-Hill, 1985; 387–397.
31. Bottomly PA. Spatial localization in NMR spectroscopy in vivo. Ann N Y Acad Sci 1987; 508:333–348.
32. Brown TR, Kincaid BM, Ugurbil. NMR chemical shift imaging in three dimensions. Proc Natl Acad Sci U S A 1982; 79: 3523–3526.
33. Maudsley AA, Hilal SK, Perman WH, Simon HE. Spatially resolved high resolution spectroscopy by "four dimensional" NMR. J Magn Reson 1983; 51:147–152.
34. Moonen CTW, Sobering G, van Zijl PCM, Gillen J, Daly P. Clinically feasible, short-echo-time proton spectroscopic imaging in three dimensions (abstr). In: Book of abstracts; Society of Magnetic Resonance in Medicine 1990. Berkeley, Calif: Society of Magnetic Resonance in Medicine, 1990; 139.
35. Hugg JW, Matson GB, Twieg DB, Maudsley AA, Sappy-Marinier D, Weiner MW. 31-phosphorus MR spectroscopic imaging (MRSI) of normal and pathological human brains. Magn Reson Imaging (in press).
36. Luyten PR, Marien AJH, van Gerwen PHJ, den Hollander JA. Localized 1H NMR

spectroscopic imaging of the human brain at 1.5 T (abstr). In: Book of abstracts; Society of Magnetic Resonance in Medicine 1990. Berkeley, Calif: Society of Magnetic Resonance in Medicine, 1990; 1060.
37. Spielman D, Meyer C, Macovski A. 1H spectroscopic imaging in the human brain using spectral-spatial excitation pulses (abstr). In: Book of abstracts; Society of Magnetic Resonance in Medicine 1990. Berkeley, Calif: Society of Magnetic Resonance in Medicine, 1990; 1061.
38. Patt SL, Sykes BD. T1 water eliminated Fourier transform NMR spectroscopy. Chem Phys 1972; 56:3182–3184.
39. Gabel RA, Roberts RA. Signals and linear systems. New York: Wiley, 1980.
40. Maudsley AA, Elliott MA, Weiner MW. Spectroscopic imaging display and analysis. Magn Reson Imaging (in press).
41. Bottomley PA, Drayer BP, Smith LS. Chronic adult cerebral infarction studied by phosphorus NMR spectroscopy. Radiology 1986; 160:763–766.
42. Sappey-Marinier D, Hubesch B, Matson GB, Weiner MW. Decreased phosphorus metabolite concentrations and alkalosis in chronic cerebral infarction. Radiology 1992; 182:29–34.
43. Brant-Zawadzki M. Ischemia. In: Stark DD, Bradley WG Jr, eds. Magnetic resonance imaging. St Louis: Mosby, 1988; 299–315.
44. Hakim AM. The cerebral ischemic penumbra. Can J Neurol Sci 1987; 14:557–559.
45. Kelly JP. Reactions of neurons to injury. In: Kandel ER, Schwartz J, eds. Principals of neural science. 2nd ed. New York: Elsevier, 1985; 187–195.
46. Karnovsky ML. Metabolic basis of phagocytic activity. Phys Rev 1962; 42:143–168.
47. Tofts PS. The noninvasive measurement of absolute metabolite concentrations in vivo using surface-coil NMR spectroscopy. J Magn Reson 1988; 80:84–95.
48. Frahm J, Michaelis T, Merboldt KD, et al. Localized NMR spectroscopy in vivo: progress and problems. NMR in Biomed 1989; 2:188–195.
49. Roth K, Hubesch B, Meyerhoff DJ, et al. Noninvasive quantitation of phosphorus metabolites in human tissue by NMR spectroscopy. J Magn Reson 1989; 81:299–311.
50. Luyten PR, Groen JP, Vermeulen JWAH, den Hollander JA. Experimental approaches to image localized human ^{31}P NMR spectroscopy. Magn Reson Med 1989; 11:1–21.
51. Segebarth CM, Baleriaux DF, de Beer et al. ^{1}H image-guided localized ^{31}P MR spectroscopy of human brain: quantitative analysis of ^{31}P MR spectra measured on volunteers and on intracranial tumor patients. Magn Reson Med 1989; 11:349–366.